



Deformation characteristics of sands in unloading

Antone Dabeet

University of British Columbia, Vancouver, BC, Canada

Dawn Shuttle

Consultant, White Rock, BC, Canada

ABSTRACT

The behaviour of sands during loading has been studied in great detail. However, little work has been devoted to understanding the response of sands in unloading. In this paper a series of drained triaxial testing on Erksak sand with load-unload-reload cycles are plotted in a stress-dilatancy framework to investigate deformation characteristics of sand during unload/reload. Contrary to the typically assumed elastic behaviour of volume increase during unloading, contraction during unloading was often observed. The magnitude of this contraction was significant for the case where soil dilated in a previous loading phase.

RESUME

Le comportement du sable pendant le chargement a été précisément étudié. Pourtant, peu d'études ont été consacrées à la réaction du sable pendant son déchargement. Dans cette étude, une série d'expériences sur du sable Erksak ont été menées dans un cadre de contrainte-dilatation pour investiguer les caractéristiques de déformation du sable pendant le chargement-déchargement-rechargement. Contrairement à un comportement élastique typique d'un matériau lors de sa décharge, c'est-à-dire à une augmentation de son volume, on a observé des compressions à plusieurs reprises lors de la décharge du sable. L'ampleur de ces compressions était significative dans le cas où le sable avait été dilaté dans une phase de charge préalable.

1. INTRODUCTION

The behaviour of sands during loading has been studied in great detail. However, little work has been devoted to understanding the response of sands in unloading. This is surprising as the behaviour of sands in unloading is of great practical importance for earthquake engineering. Undrained cyclic simple shear tests show that the increase in pore water pressure generated during the unloading cycle often exceeds that generated during loading (Wijewickreme et. al., 2005). This tendency to contract upon unloading during an earthquake could result in liquefaction.

An elastic material is expected to expand upon unloading in a conventional triaxial test. Drained triaxial tests indicate that, contrary to the expected elastic behaviour, sand may exhibit contractive behaviour when unloaded. Drained cyclic simple shear tests show similar behaviour in unloading (Sriskandakumar, 2004). Therefore, it is clear that soil behaviour in unloading is not wholly elastic.

This work presents a series of drained triaxial tests on Erksak sand with load-unload-reload cycles. The main focus of this review of experimental results is to investigate the inter-relationship between stress and dilatancy in unloading.

1.1. Stress-Dilatancy Relations

Stress-dilatancy in soil is the relation between the stress level in the soil and the corresponding volume changes with shear. Quantitatively stress-dilatancy is usually expressed as the relation between η and D where η is

the ratio of the deviatoric stress invariant to mean effective stress (q/p') and D is the dilatancy defined as $\mathcal{E}_v / \mathcal{E}_q$ where \mathcal{E}_v and \mathcal{E}_q are the increments of plastic

volumetric strain and plastic shear strain invariant respectively. Theoretically dilatancy usually refers to the plastic strain increments, but prior to routine use of bender elements total strains were also widely used as these are directly measured in laboratory testing. For most sands the difference between total and plastic dilatancy is very small at higher stress ratios.

Stress dilatancy in loading has been the topic of much investigation. Rowe (1962) was the first to quantify stress-dilatancy during the entire stress strain curve based on his research on particle to particle interaction. Equation 1 is Rowe's stress-dilatancy for triaxial compression.

$$D^p = \frac{9(M - \eta)}{9 + 3M - 2M\eta} \quad [1]$$

$$M = \frac{6 \sin \phi_{cv}}{3 - \sin \phi_{cv}} \quad [2]$$

In Equation 2, also for triaxial compression, M is the critical friction ratio in $q-p'$ space and ϕ_{cv} is the constant volume friction angle. Reviewing experimental data, Rowe (1969) observed that constant M fits observations poorly, and a more appropriate parameter to use in Equation 1 is the mobilized friction angle M_f , where M_f is a friction ratio that changes during the test depending on

void ratio and pressure. Rowe's theoretical model is based on dissipation of work. Upon loading, work is done by the major principal stress on an assembly of soil particles. The model assumes that part of this work is dissipated in friction. The assembly transfers the remaining part as work done in the minor principal stress direction.

Schofield and Wroth (1968), considering soil as a continuum, defined a dilatancy rule for the Cam-Clay critical state soil model (Equation 3).

$$D^p = M - \eta \tag{3}$$

Cam-Clay is widely used for soft clay, but the dilatancy rule does not match sands data well, particularly for dense sands. Nova addressed this issue in 1982 and developed an improved stress-dilatancy rule based on observations from lab data (Equation 4). Nova's equation contains an additional volumetric coupling parameter (N) which usually falls in the range of 0.2-0.4.

$$D^p = \frac{(M - \eta)}{(1 - N)} \tag{4}$$

Figure 1 plots the Rowe, Cam-Clay and Nova flow rules for $M=1.27$ and $N=0.25$. It is noteworthy that the trends are fairly similar in the dilatant range (i.e. for negative D^p) for a typical critical friction ratio of 1.27 (i.e. $\phi_{cv} = 31.6^\circ$).

Less work has been done on stress-dilatancy in unloading. Jefferies (1997) derived an equation for stress-dilatancy in unloading based on the assumption that soil stores 'plastic' energy in loading that is recovered upon unloading. Starting from Nova's flow rule, and substituting for D^p and η (i.e. $\frac{\epsilon_v^p}{\epsilon_q^p}$ and q/p' , respectively) in Equation 4 and expanding yields:

$$q\frac{\epsilon_v^p}{\epsilon_q^p} + p\frac{\epsilon_v^p}{\epsilon_q^p} = Mp\left|\frac{\epsilon_v^p}{\epsilon_q^p}\right| + Np\frac{\epsilon_v^p}{\epsilon_q^p} \tag{5}$$

The terms on the left hand side of Equation 5 represent plastic work done. The right hand side represents what soil does with that work. The first term on the right hand side represents energy dissipation (Schofield and Wroth, 1968). The second term on the right hand side represents 'plastic' energy stored in loading and recovered in unloading (Jefferies, 1997). The saw tooth model gives a simple physical explanation of 'plastic' energy storage. Accordingly, the potential energy of individual soil particles is increased in loading as the particles assume new locations. This energy is released upon unloading as the particles tend to recover their original locations before loading. This is associated with contractive response in unloading. For the unloading phase, $\frac{\epsilon_v^p}{\epsilon_q^p} < 0$ and the N term in Equation 5 takes a negative sign as it represents 'plastic' energy recovered. Substituting and rearranging gives Equation 6 for stress-dilatancy in unloading. Equation 6 is plotted in Figure 2.

$$D^p = \frac{-M - \eta}{1 + N} \tag{6}$$

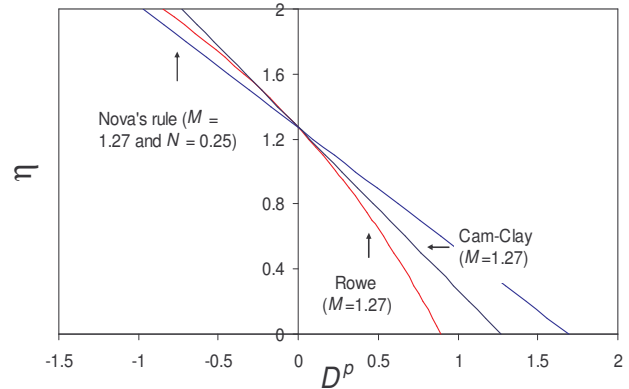


Figure 1. Rowe, Nova and Cam-Clay stress-dilatancy relations for loading.

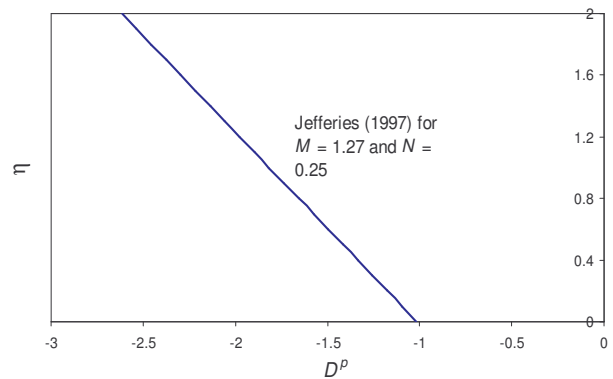


Figure 2. Jefferies stress-dilatancy relation for unloading.

2. TESTING PROGRAM

2.1. Sand Tested

The testing of Erksak 330/0.7 sand, a sand comprehensively investigated in the 1980's when it was used for construction of the Molipak in the Canadian Arctic, has been used for this work. Erksak 330/0.7 has an average particles size of 330 μm and fines content of 0.7%. It is a uniformly graded (uniformity coefficient = 1.8) medium-grain sub-rounded sand mainly composed of quartz and feldspar. Its specific gravity is 2.66. The minimum and maximum void ratios, e_{min} and e_{max} , measured according to ASTM 1988a and ASTM 1988b, are 0.525 and 0.775, respectively (Sasitharan 1989).

2.2. Testing Program

All tests reported in this paper were undertaken by Golder Associates and the data can be downloaded from (www.golder.com/liq). The testing program included 29 drained and 39 undrained triaxial tests. As this investigation focuses on volumetric changes drained tests were of primary interest. The ten drained tests that

followed a conventional triaxial stress path and also contained load-unload-reload cycles were used for this work. The principal stress direction for these tests is constant during the cyclic loading. The effect of principal stress rotation on stress-dilatancy is outside the scope of this paper.

The tests covered a wide range of mean effective stresses (100-800 kPa) with void ratios ranging from 0.603 to 0.723 (see Table 1). All samples were water pluviated, except for ES_CID_868 which was moist tamped. The number of unload-reload loops varied with a maximum of three loops in any test. Some of the loops occurred before reaching peak strength, while others occurred post-peak.

Table 1. Drained triaxial compression tests on Erksak sand (data from www.golder.com/liq).

Test ¹	p' (kPa)	e_o	No. of U-R loops ²
ES_CID_860	100	0.672	1
ES_CID_861	100	0.645	2
ES_CID_862	100	0.645	3
ES_CID_866	400	0.698	2
ES_CID_867	400	0.680	3
ES_CID_868	400	0.723	2
ES_CID_870	800	0.653	1
ES_CID_871	800	0.637	2
ES_CID_872	800	0.652	3
ES_CID_873	100	0.603	3

¹All tests were water pluviated apart from ES_CID_868 which was moist tamped.

²U-R stands for unload-reload.

3. EXPERIMENTAL OBSERVATIONS

In the following discussion “U” refers to an unloading loop and “L” refers to a loading or reloading loop. The number following the symbol denotes the order of a particular loop from the beginning of the test. Positive volumetric strains are contractive and negative volumetric strains are dilative.

3.1. Effect of Unload-Reload Loops on Strength and Volumetric Strains

A typical test is plotted in Figure 3. The strength of the sand, plotted in Figure 3a as stress ratio η ($=q/p'$) versus axial strain ϵ_1 , does not seem to be highly affected by the unload-reload loops. The data shows that prior to reaching image condition (coincident with the boundary between contractive and dilative behaviour) the effect of an unload-reload loop on the overall stress-strain curve is minimal as shown in Figure 3a. Loading following loop U1 shows increasing stress ratio with strain as if the unload-reload loop did not exist (there is no local peak in the $\eta - \epsilon_1$ curve). Conversely, small peaks are seen following the unload-reload loops for the cases where those loops occur at post-image strain conditions. For example, loops U2 and U3 (post-image loops) are followed by small local peaks in the $\eta - \epsilon_1$ curve. The local peaks are more easily

observed in a shear stress vs. axial strain, as shown in Figure 4 for the same test (ES_CID_867). Other tests on Erksak sand demonstrate similar behaviour.

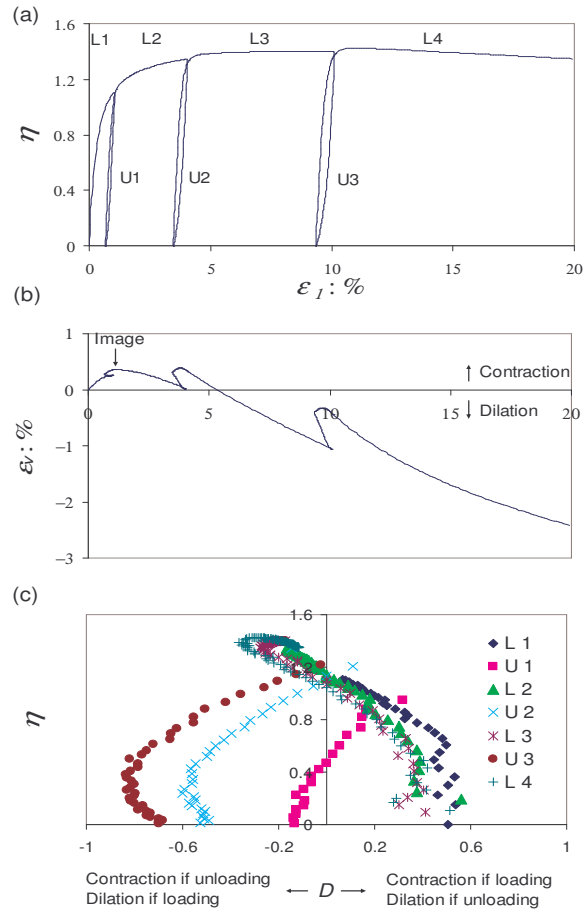


Figure 3. Data from ES_CID_867 (a) stress ratio vs. axial strain (b) volumetric vs. axial strain (c) stress ratio vs. dilatancy.

Conversely, volumetric strains are dramatically influenced by the unload-reload loops. Both the absolute values and the rates of change are affected (Figure 3b). Unloading occurs starting from pre-image stress ratio for U1. Note that volumetric changes associated with unloading are very small and are initially contractive followed by a small dilative phase (see Figure 5a for an enlarged view). However, for U2 and U3 the volumetric changes associated with unloading are significant and are dominantly contractive (see Figure 5b for a zoom on U2). It is noteworthy that unloading for those two loops starts from a post-image stress ratio.

The effect of the number of unload-reload loops is illustrated using tests ES_CID_870 and ES_CID_872 which have similar e_o and initial p' . The only difference is that the former has one unload-reload loop while the later has three loops. Figure 6a shows that the difference in the number of loops has only a small effect on the stress ratio vs. axial strain plot. The first loop in ES_CID_872 causes only a small change in volumetric strains while the

second loop causes significant contraction when compared to the results of ES_CID_870 (Figure 6b). Note that the first loop in ES_CID_872 is pre-image while the second is post-image. In the third loop, both tests start from approximately similar points and demonstrate similar behaviour. It can be noticed that the volumetric strain curve for ES_CID_872 after the second loop is steeper than that for ES_CID_870. This implies that the unloading loop influences volumetric changes patterns in subsequent reloading and therefore stress-dilatancy in reloading changes.

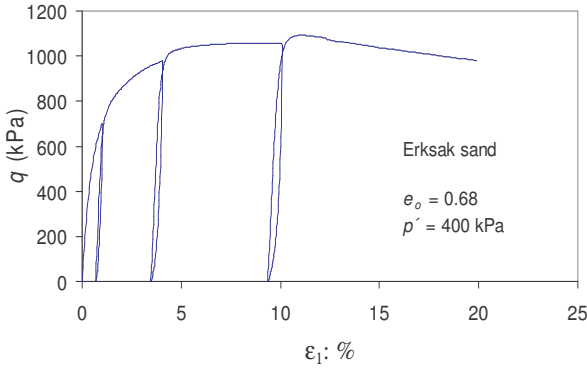


Figure 4. Data from ES_CID_867 in shear stress vs. axial strain.

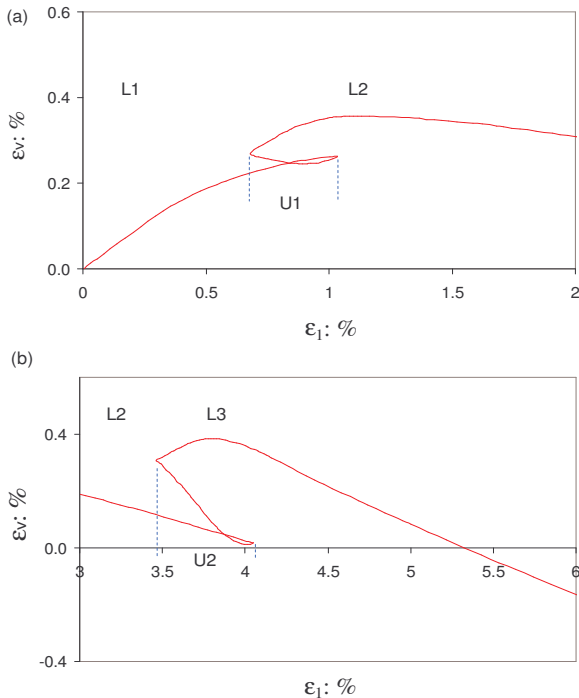


Figure 5. Zoom on loops 1 (a) and 2 (b) for ES_CID_867.

The stress-strain and volumetric strain curves for tests ES_CID_861 and ES_CID_862 are very similar (Figure 7). The two tests have identical e_o and initial p' . The first

has two unload-reload loops while the second has three unload-reload loops. The additional loop in ES_CID_862 is pre-image and therefore does not cause any significant difference between the results of the two tests.

In all tests reported in Table 1, if unloading starts from a post-image stress ratio, volumetric strains are significant and are either totally contractive or dominated by contraction (Dabeet, 2008). Conversely, if unloading starts from pre-image stress ratio, volumetric strains are small and are either totally dilative or dominated by dilation.

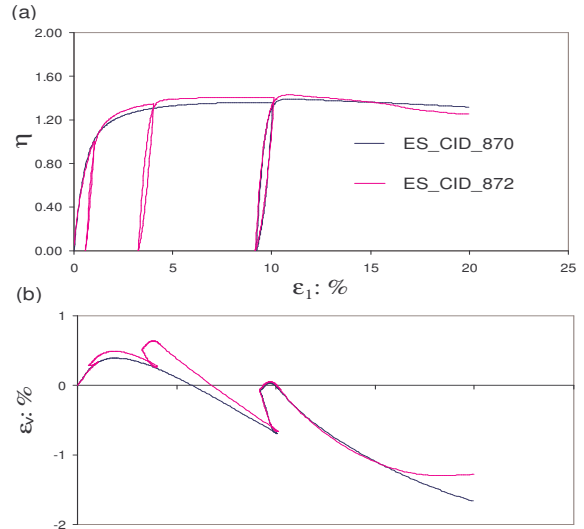


Figure 6. Tests ES_CID_870 and ES_CID_872 with similar e_o and initial p' but different number of U-R loops (a) axial strain vs. stress ratio (b) axial strain vs. volumetric strain.

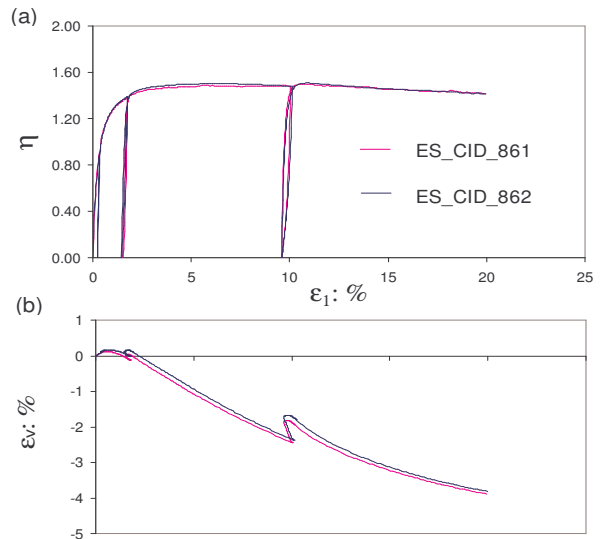


Figure 7. Tests ES_CID_861 and ES_CID_862 with similar e_o and initial p' but different number of U-R loops (a) axial strain vs. stress ratio (b) axial strain vs. volumetric strain.

3.2. Effect of Stress Ratio at Unloading on Dilatancy

The effect of stress ratio on dilatancy during unloading is illustrated in Figure 3c, which presents the same data as for Figures 3a & 3b, but now plotted in stress-dilatancy space. The following equation was used to calculate dilatancy from lab data:

$$D_n = \frac{\epsilon_{v(n+1)} - \epsilon_{v(n-1)}}{\epsilon_{q(n+1)} - \epsilon_{q(n-1)}} \quad [7]$$

where n denotes the current measurement. For the case of unloading, positive dilatancy means volume increase while negative dilatancy indicates volume decrease.

Figure 3c shows that pre-image unloading response is dominated by dilation while post-image unloading is dominated by contraction. For unload phases U2 and U3, the sample contracts except for one U2 measurement. Unloading for U2 and U3 starts from a post-image (dilative) stress ratio. Conversely U1 is unloaded from a pre-image (contractive) stress ratio, and it increases in volume in the beginning of the unloading phase. U1 then starts contracting towards the end of the unloading phase.

This behaviour shows that soil does not unload in an elastic manner for U2 and U3. That the behaviour of U2 and U3 is not elastic is known for two reasons: 1) dilatancy is constant for elastic behaviour 2) measured dilatancy is negative which is not possible under the elastic framework for the conventional triaxial stress path. For U1, where the sample is unloaded from a pre-image stress ratio, there is a small elastic part represented by the first three points in the dilatancy plot. However, there is some uncertainty in interpretation because of the small number of data points. The elastic part is followed by plastic yielding. It can be seen from Figure 3c that the dilatancy in unloading plots are approximately perpendicular to those for loading.

The position of stress-dilatancy curves in unloading is seen to depend on the stress ratio at which previous loading stopped. For example, the last value of stress ratio for L2 is greater than that for L1. The y-intercept of U2 (subsequent to L2) is greater than that for U1 (subsequent to L1).

3.3. Effect of Fabric

Similar behaviour is observed for the moist tamped sample, test ES_CID_868 (Figure 8). Significant contraction is observed for U1 and U2 (Figure 8b). Both loops start post-image (U1 starts from $\eta = 1.212$ and image for L1 is at $\eta = 1.209$). Stress-dilatancy plots in unloading are almost perpendicular to those in loading (see Figure 8c). The stress ratio at the end of loading is directly related to the amount of contraction in subsequent unloading (U2 is associated with more contraction than U1). The previously described behaviour of sand seems to be independent of the sample preparation method.

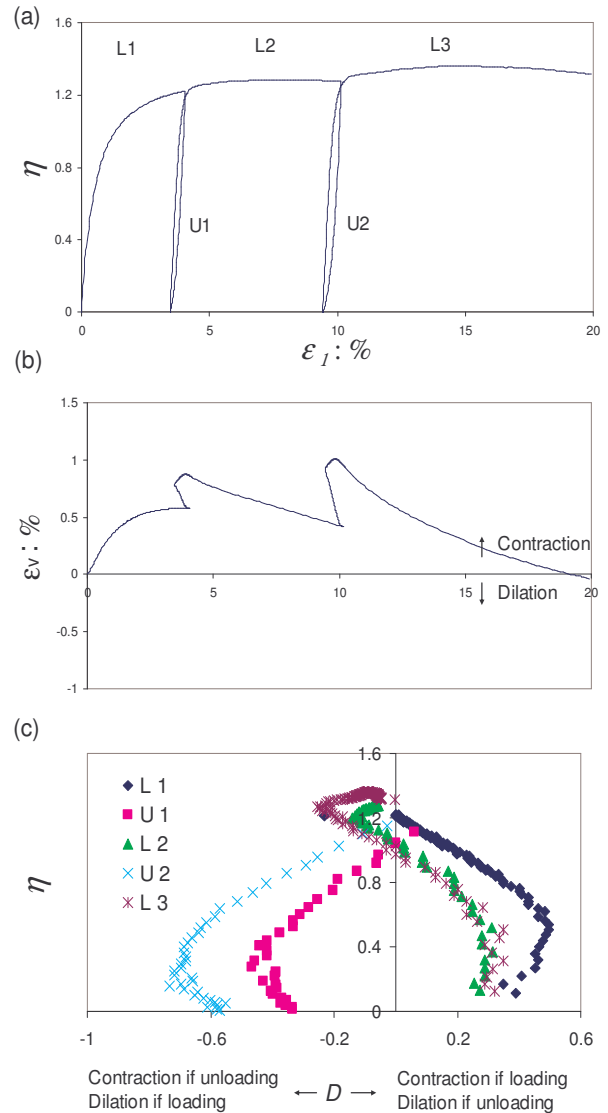


Figure 8. Data from ES_CID_868 (a) stress ratio vs. axial strain (b) volumetric vs. axial strain (c) stress ratio vs. dilatancy.

4. IMPLICATIONS OF EXPERIMENTAL OBSERVATIONS

An elastic material expands in response to a decrease in mean effective stress. The observed deformation characteristics during unloading are highly dependent on the stress ratio at the start of unloading (or the end of previous loading). If this stress ratio is less than that at image, unloading is dominated by a small amount of dilation. However, once the image stress ratio is exceeded, unloading is associated with significant amount of contraction. This indicates inelastic behaviour or 'yield in unloading'. Therefore, it appears that the

image condition defines the first possible location where yield in unloading can occur. This is equivalent to stating that yield in unloading must occur at a post-image location, and that dilation in loading is a prerequisite for significant contraction in unloading. This contradicts most soil models where unloading is inside the yield surface and is elastic.

Contraction due to post-image unloading can be explained based on the saw-tooth model. When stress ratio exceeds that for image, the sample starts to dilate. It stores potential energy that can be recovered in the form of contraction in unloading (Jefferies, 1997). If dilation can be thought of as soil particles sliding on top of each other, then a situation similar to that of the sawtooth model shown in Figure 9a develops in loading. Upon unloading, which can be thought of as pushing the upper part of the sawtooth to the left, the particles would tend to slide back to their original location prior to loading (Figure 9b). This is associated with contraction. Therefore, plastic dilation in loading is responsible for the observed contraction in subsequent unloading.

The model suggests that the amount of contraction in unloading is related to the amount of dilation in the previous loading. The more soil dilates in loading, the more potential energy is stored that is available to be released as contraction in subsequent unloading. This matches the observed trends from the Erksak laboratory data.

It was shown in Section 3.1 that post-image unload-reload loops demonstrate a new peak in stress-strain curves. This is consistent with the behaviour that post-image unloading is associated with contraction and a denser soil is expected to have higher peak strength.

Equation 6 plotted in Figure 2 predicts different trends (more contraction in unloading) than those observed from lab data (see Figures 3c & 8c). The expression assumes that all 'plastic' energy stored in a loading phase must be released in the subsequent unloading phase which does not seem to be the case (i.e. only part of this energy is released in the subsequent unloading phase).

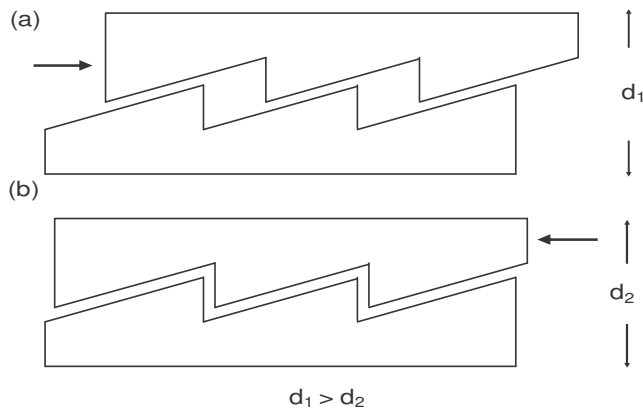


Figure 9. The saw-tooth model for dilatancy in (a) loading (b) unloading

5. CONCLUSION

The study of ten drained conventional triaxial tests on Erksak sand, including between one and three unload-reload loops, indicate that significant amounts of contraction occur during unloading. This is contrary to the dilatant elastic unloading response often assumed in constitutive models of soil.

Experimental observations indicate that unloading loops starting from pre-image stress ratio are dominated by small amounts of dilation, while those starting from post-image stress ratio are dominated by significant amounts of contraction. The effect of the unload-reload loops on peak strength is small.

This observed contraction in unloading can be explained based on the saw-tooth model. The sawtooth model suggests that the more soil dilates in loading, the more potential energy the soil stores. This energy is available to be released as contraction in subsequent unloading, as observed experimentally.

ACKNOWLEDGEMENTS

The authors would like to thank the University of British Columbia Graduate Fellowship for providing funding for this research. The authors would also like to acknowledge Golder Associates for providing access to the laboratory testing on which this research is based.

NOTATION

M	critical friction ratio (q/p' at critical state)
N	volumetric coupling parameter
p'	mean effective stress $(\sigma'_1 + 2\sigma'_3)/3$
q	shear stress $(\sigma'_1 - \sigma'_3)$
ϵ_1	axial strain
ϵ_3	radial strain
ϵ_v	volumetric strain $(\epsilon_1 + 2\epsilon_3)$
ϵ_q	shear strain for triaxial compression $2(\epsilon_1 - \epsilon_3)/3$
η	stress ratio (q/p')

Dot over a symbol denotes increments, 'o' subscript denotes initial, and 'p' superscript denotes plastic.

REFERENCE

- ASTM. 1988a. Standard test methods for maximum index density of soils using a vibratory table (D4253-83), in *1998 Annual Book of ASTM Standards*, 4.08: 554-565.
- ASTM. 1988b. Standard test methods for minimum index density of soils and calculation of relative density (D4254-83), in *1998 Annual Book of ASTM Standards*, 4.08: 566-572.
- Dabeet. 2008. A practical model for load-unload-reload cycles on sand, M.A.Sc Thesis, University of British Columbia, Vancouver, BC, Canada.

- Golder Associates. Erksak 330/0.7 triaxial tests, available at www.golder.com/liq.
- Jefferies, M. 1997. Plastic work and isotropic softening in unloading, *Geotechnique*, 47: 1037-1042.
- Nova, R. 1982. A constitutive model for soil under monotonic and cyclic loading, in *Soil Mechanics Transient and Cyclic Loads*, Wiley, New York, USA.
- Rowe, P. W. 1962. The stress-dilatancy relation for static equilibrium of an assembly of particles in contact, *Proceedings of the Royal Society, UK*, A269: 500-527.
- Rowe, P. W. 1969. The relation between the shear strength of sands in triaxial compression, plane strains and direct shear, *Geotechnique*, 19: 75-86.
- Schofield, A. and Wroth, C. 1968. *Critical state soil mechanics*, McGraw Hill, London.
- Sasitharan, S. 1989. Stress path dependency of dilatancy and stress-strain response of sand, M.A.Sc Thesis, University of British Columbia, Vancouver, BC, Canada.
- Sriskandakumar, S. 2004. Cyclic loading response of Fraser River sand for validation of numerical models simulating centrifuge tests, M.A.Sc Thesis, University of British Columbia, Vancouver, BC, Canada.
- Wijewickreme, D. Sriskandakumar, S. and Byrne, P. 2005. Cyclic loading response of loose air-pluviated Fraser River sand for validation of numerical models simulating centrifuge tests, *Canadian Geotechnical Journal*, 42: 550-561.